

OPTIMUM DESIGN OF A HYBRID ISOLATION DEVICE FOR SERVER RACKS USING CONSTRAINED DIFFERENTIAL EVOLUTION ALGORITHM

Luca Aceto¹, Giuseppe Quaranta², Guido Camata¹, Bruno Briseghella³, Enrico Spacone¹

¹ Department of Engineering and Geology
University G. D'Annunzio of Chieti-Pescara
Viale Pindaro 42, 65127 Pescara, Italy
e-mail: luca.aceto@unich.it, guido.camata@unich.it, enrico.spacone@unich.it

² Department of Structural and Geotechnical Engineering
Sapienza University of Rome
Via Eudossiana 18, 00184 Rome, Italy
e-mail: giuseppe.quaranta@uniroma1.it

³ College of Civil Engineering
Fuzhou University
Fuzhou 350108, China
e-mail: bruno@fzu.edu.cn

Abstract

Nonstructural elements and contents often constitute a large fraction of the economic investment in ordinary buildings. In case of seismic events, damage to nonstructural elements not only contributes to the overall direct material costs but can also significantly impact the indirect costs. The latter are especially affected by earthquake-induced damage if production and business flows depend on proper functioning of such nonstructural components, since consequent downtime costs turn out to be very high. Within this framework, server racks' performance under seismic loading is of interest in the present work. The economic relevance of these nonstructural components requires the implementation of proper design solutions so that their performance under earthquakes can fulfill specific requirements. In this perspective, including isolation devices between server racks and building floors is deemed effective for enhancing the stability of the protected equipment, preserving the computer components' integrity and, minimizing downtime losses. Hence, the present work is meant to optimize a hybrid isolation system for server racks. Specifically, the hybrid isolation device designed for such application combines at least two elastomeric isolators and three sliders, and it is intended for the seismic protection of server racks characterized by different configurations. The objective function is formulated to minimize the accelerations transmitted to server racks and manufacturing cost.

Keywords: Constrained optimization – Cost minimization – Nonstructural elements – Optimum structural design – Server rack – Seismic isolation

1 INTRODUCTION

Nonstructural elements and contents contribute to large part of the initial economic investments in typical buildings, but they often undergo disproportional damage due to seismic actions even if the structure in which they are placed exhibits satisfactory performances [1]. Apart from contributing directly to final material costs after an earthquake, damage to contents housed in most buildings can cause inestimable losses (in case of objects of historical value) or the interruption of production/business flows (when damage occur in industrial equipments, computer servers, etc.) along with extremely high downtime costs. For example, the economic cost due to the five-days of downtime for a single data center following the 1989 Loma Prieta earthquake or the 1994 Northridge and 1995 Kobe seismic events amounted to 5%-10% of the entire rebuilding cost [2]. In this regards, it is opportune to point out that many building contents – such as computer servers or museum artifacts – are acceleration-sensitive, i.e., they are especially vulnerable to damage when subject to high accelerations [3]. In this perspective, there has been growing interest about the use of seismic isolators at the floor level because, in most cases, this can cope efficiently with the need of protecting acceleration-sensitive building equipments under earthquake, provided that the building structure is properly designed against seismic loads. In fact, it is recognized that seismic isolation of server racks would improve business resiliency at a low cost as compared to downtime losses [4].

Within this framework, the present paper proposes a novel design procedure in order to optimize a hybrid isolation system for server racks combining at least two elastomeric isolators and three sliders. The objective function is selected to minimize the accelerations transmitted to the servers placed in the racks as well as the material cost of the isolation system. Design variables include number, compound, and geometric dimensions of the elastomeric elements and slider position. The final optimization problem is then solved using a suitable variant of the differential evolution algorithm [5] to handle the design constraints. The search for the optimal hybrid isolation system is carried out in two phases. The first phase is concerned with the identification of the optimal device to be deployed on all floors of a given building. The standardized optimal design is addressed next in the second phase, in which the design procedure is extended to determine which isolation device is best suited for all floors of the building stock under investigation. The sliders optimal topology is also investigated parallel to that in such a way to minimize the overturning moment. This final design phase is motivated by the fact that standardization and generalization of an industrial device during the development stage are crucial to reduce engineering and production costs. As a matter of fact, they allow to circumvent the redesign phase should any design condition changes and to reduce the costs related to the acceptance tests required in the development stage. Hence, it means no waste of any other devices except the installed ones, thereby saving materials and overall unitary industrial costs.

2 OVERVIEW ABOUT COMMON PRACTICES IN DATA CENTER DESIGN

Most of the world's largest data centers are housed within dedicated one-story buildings, which usually host some offices serving as technical or control rooms. Medium to large data centers are often located within the upper floor of a commercial building. The position of small data centers can vary considerably in terms of, both, building type and location within the host structure. Standard models exist for large data centers placement only, whereas they lack for small to medium-large ones [6].

The distribution of racks in the data center varies significantly, regardless of the size. The most common racks configuration in large data centers is based on rows of racks installed side-by-side with alternating cold aisles and hot aisles [7]. Generally, the rows of racks are placed back-to-back, and all the holes through the rack are blocked off to create barriers that reduce

recirculation and divide hot aisles from cold aisles efficiently [8]. In some cases, hot aisles or cold aisles between two rows of racks are covered with a modular system of cooling containment. This choice reduces the energy cost and concentrates the refrigerated airflow on the rack when the server room is vast or the inter-floor space is large enough compared to the vertical dimension of the racks [9].

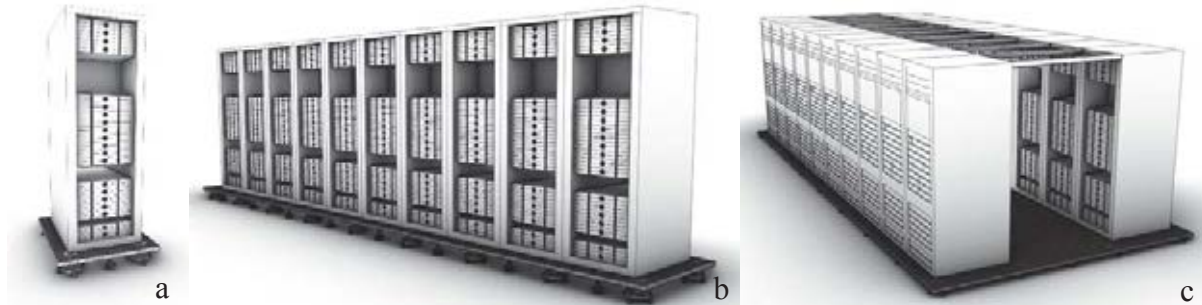


Figure 1 – Most common server racks configurations: a) single rack; b) row of racks; c) rows of racks with covered aisle.

The aisle containment system is composed of a series of light aluminum frames that do not have a structural function. Generally, these systems are scalable, and thus there is no a fixed number of racks that compose the covered aisle. Server rooms can host multiple rows of racks and multiple covered aisles.

Data center density is usually measured in terms of W/m^2 or $W/rack$, which represent the electric power consumed per square meter and the electric power consumed per rack, respectively. It means that a low-density data center is characterized by a configuration that consumes few Watts per square meter of the server room. If a data center employs this configuration, then the rows are commonly composed of sparsely populated racks or spaced full single racks [10].

As reported in many guidelines, scalability brings added value to the data center. The scalability requirement implies that the data center can be conceived and built according to a low-density architecture able to meet current needs and to expand for fulfilling higher future demands that require the postponed installation of further infrastructures such as UPS systems, air conditioners, and other racks [10]. This means that the data center layout can eventually evolve during its lifetime, with the possible exception of large and predefined configurations.

It is anticipated that this study addresses the seismic protection of a single rack, whereas the remaining configurations will be considered in future works. The configuration consisting of a single rack device is the most flexible one and facilitates later installations when data center scaling is needed. Some available commercial proposals for server rack seismic isolation are intended for a single item. They are generally modular systems, which means that it is possible to isolate more racks in a row by combining more devices [11–19]. Many other commercial devices propose total raised floor isolation [13,19,20]. Another solution adopted to achieve server rack seismic protection is obtained through the direct introduction of damping to the rack's steel structure or in the raised floor [21,22]. The main guidelines and codes that refer to electronic equipments installed in earthquake-prone areas suggest the use of a cabinet rack that has passed a codified seismic test, usually named "seismic rack" [23–30]. On the other hand, to make a non-conforming cabinet resistant against seismic actions, the installation of a "seismic kit" composed of steel braces is common. Both solutions are meant to enhance the rack resistance and stiffness. Furthermore, technical codes in force indicate that racks in seismic areas have to be anchored to the floor by fasteners together with shear keys. Although these specifications already existed during the 2010 Chile earthquake, the lack of fasteners and shear keys

was common in both new and old buildings [31]. It is worthy highlight that code requirements that target at increasing the system stiffness to reduce the drift generally lead to an increment of the acceleration demands in the electronic components of the racks, thereby amplifying the potential risk of interrupting the business continuity.

3 ANALYSIS OF ELASTOMERIC ISOLATORS

Design rules provided by EN 15129 [32] and EN 1337-3 [33] for seismic actions and static conditions, respectively, are the constraints of the optimization procedure.

The use of slender elastomeric elements is required to ensure a suitable level of isolation for light nonstructural elements. This condition turns out to be very binding for axial loads, since it makes elastomeric elements vulnerable to buckling phenomena. In order to overcome this issue, a hybrid isolation system is adopted, which combines elastomers with at least three sliders that aims at absorbing the axial load. Thanks to these features, elastomeric elements integrity under seismic loads is governed primarily by shear deformability limits. In operating conditions, the racks positioned inside the building are protected against horizontal environmental actions, such as wind. Therefore, only an accidental rotation equal to 0.03 rad and a horizontal force equal to 1 kN are considered during the optimization procedure to account for anthropic interferences. According to EN 15129, the design shear strain $\varepsilon_{q,E}$ due to earthquake-imposed design displacement d_{bd} is given by:

$$\varepsilon_{q,E} = \frac{d_{bd}}{T_q}, \quad (1)$$

where T_q is the total thickness of the active elastomer during shear. The design shear strain calculated using Eq. (1) has to be compared with the maximum shear strain equal to 2.5.

4 SEISMIC ACTION

The floor response spectrum method is a convenient way to find the nonstructural element acceleration on the floor during an optimization procedure because it is less computationally expensive than a time history analysis [34]. The Italian building code (NTC18) floor spectrum formulation [35] is here employed, which demonstrated a good agreement with the Newmark response spectrum derived from a compatible time history analysis.

According to NTC18, the seismic demand on nonstructural elements can be determined by applying a horizontal force F_a defined as follows:

$$F_a = \frac{(S_a \cdot W_a)}{q_a}, \quad (2)$$

where F_a is the horizontal seismic force applied in the center of mass of the nonstructural element, S_a is the maximum dimensionless acceleration, W_a is the weight of the element, and q_a is the quality factor. The following relationship is adopted to determine the acceleration at the j th floor of the structure corresponding to the i th mode:

$$S_{ij} = \varphi_{ij} \Gamma_i S_i(T_i), \quad (3)$$

where $S_i(T_i)$ is the ordinate of the spectrum relative to the i th mode. Herein, Γ_i is the modal participation factor, which is defined by the relationship:

$$\Gamma_i = \frac{\varphi_i^T M \tau}{\varphi_i^T M \varphi_i}, \quad (4)$$

where τ is the drag vector, φ_i is the i th normalized modal shape, and M is the mass matrix.

A ground spectrum for a high seismic risk zone with $a_g=0.26g$ is considered in the present work (Figure 2a). Additionally, it is assumed that the building containing the racks has to undergo slight damage levels or to behave elastically; otherwise, business continuity would be jeopardized in any case. Therefore, the design of the isolation system will not rely on the ductility reserve that the structure would provide by adopting a unit quality factor.

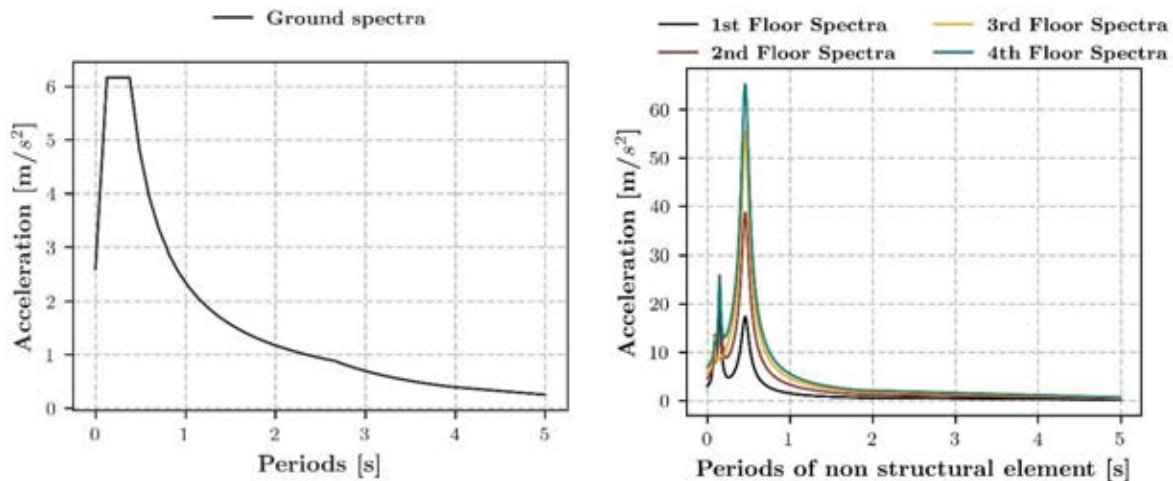


Figure 2 – Reference ground spectrum (left) and floor spectra for a 4-story building (right).

The floor spectra for ten buildings with an increasing number of floors were generated accordingly. As an example, the floor spectra for a 4-story building are shown in Figure 2b. All buildings have a concrete frame structure and $5\text{ m} \times 5\text{ m}$ square floor plan with an inter-floor height equal to 3.5 m. The first frame is replicated to obtain all buildings (Figure 3).



Figure 3 – Stock of buildings under consideration.

5 OPTIMIZATION PROCEDURE

The optimization problem is formulated, taking into account both, integrity of the isolated servers and system cost-effectiveness. Within the present work, the elastomeric isolator's behavior and the seismic actions are evaluated through an iterative search considering the mechanical characteristics of the elastomeric compound and the floor response spectra for each floor. The elastomer's lateral stiffness was calibrated by considering the damping related to the shear deformation calculated through the floor spectral displacement until convergence. The optimization procedure is divided into two phases. In the first phase, the optimum isolation system is identified separately for the ten buildings under consideration (Figure 4). Thus, for each candidate solution generated by the differential evolution algorithm, the iterative procedure required to identify the isolation system's properties was conducted for each floor of the

considered building. In the second phase, all ten buildings are examined simultaneously in the attempt to determine the optimal isolator that complies with all constraints on all floors of all buildings. In this case, the isolator properties were identified for all floors of the ten buildings for each generation. The design variables in the optimization problem are diameter of the elastomeric isolators, rubber height, type of compound, and number of isolators. From these quantities, it is thus possible to derive number of rubber layers and number of steel layers for the isolator. The algorithm employs primary and derived design variables in order to calculate the material cost of the isolation system. The problem constraints are defined in compliance with the design rules in EN 1337-3 and EN 15129. Furthermore, the maximum acceleration at the top of the rack is required to be less than 0.20g, whereas the isolation system period is forced to be larger than 1 s. The limitation about the maximum acceleration transmitted to the servers by the rack is necessary to ensure that the hard disks would remain operational during seismic events.

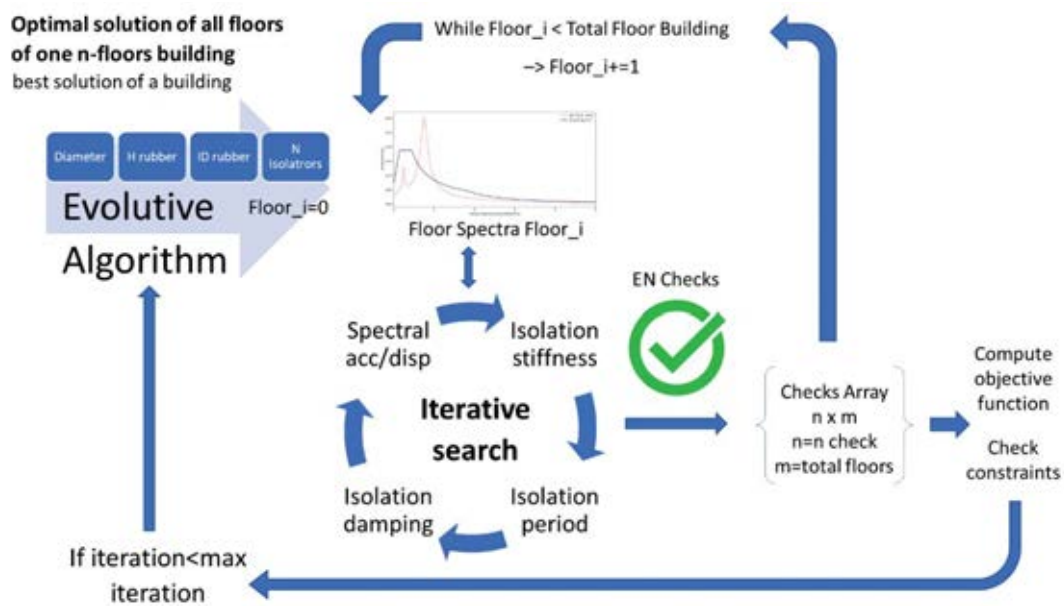


Figure 4 –Workflow of the optimization procedure for a single building

A special $(\mu+\lambda)$ -constrained differential evolution algorithm is adopted to solve the optimization problem. This algorithm uses a robust nature-inspired strategy that focuses on finding the best solution iteratively by checking a set of candidate solutions [36,37]. The objective function of the optimization problem $ObjF$ is formulated as follows:

$$ObjF = \left(\frac{C_{Mat} + C_{Fixed}}{C_{Fixed}} \right) \cdot \gamma_c + Acc_{max} \cdot \gamma_{Acc} \quad (5)$$

where C_{Mat} is the material cost of the isolation system, C_{Fix} are the fixed costs, Acc_{Max} is the maximum acceleration recorded on the floors of each building. The two terms included in the objective function are weighted using two user-defined coefficients (i.e., γ_C and γ_{Acc}). The constrained differential evolution algorithm's iterative strategy runs until the maximum number of fitness evaluations is reached. Meanwhile, the sliders position is optimized to reduce the overturning moment due to the seismic action. The only design variable is the position of the sliders as related to the dimensions of each individual rack. In this case, the optimum design is formulated as a single-objective constrained optimization problem, and the $ObjF$ $f(x_i)$ is calculated as follows:

$$ObjF = \frac{M_{Stab}}{M_{Ov}} \quad (6)$$

where M_{stab} is the stabilizing moment, and M_{ov} is the overturning moment under seismic action.

6 RESULTS

Figure 5a shows the results for all the analyses performed in the first design phase by overlaying the trends in the devices' geometric dimensions with the maximum acceleration values recorded for each building. Figure 5b illustrates the maximum acceleration among all floors of each building, and compare them to the acceleration of a floor-fixed rack. All results are listed in Table 1. A fundamental period equal to 0.33 s is considered for the non-isolated seismic rack [38]. The numerical value of the weights are $\gamma_C=3$ and $\gamma_{Acc}=0.30$ [1/g]. The optimal number of elastomeric devices was found equal to 2 for all cases (it corresponds to the lower bound).

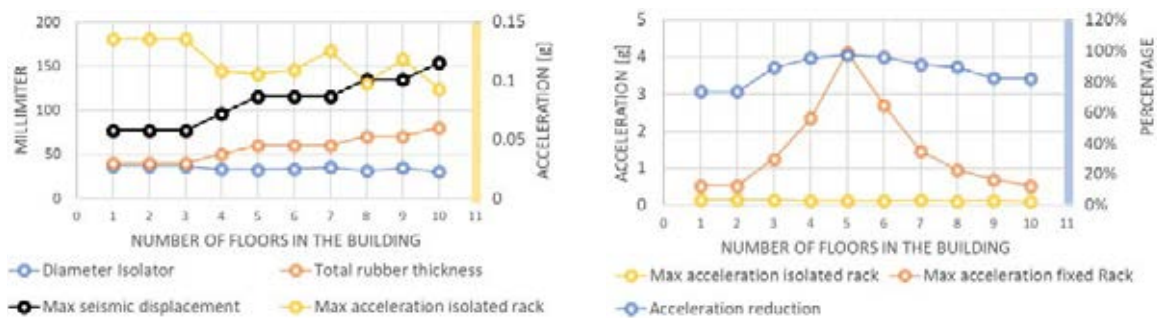


Figure 5 – Results of the optimization performed in the first phase (left) and comparison between maximum acceleration on the isolated rack and that of a fixed-floor rack (right).

Number of floors	Isolator diameter [mm]	Total rubber thickness [mm]	Cost of isolation system [€]	Objective function	Max seismic displacement [mm]	Max acceleration isolated rack [g]
1	37	40	288	1.29	77	0.1354
2	37	40	288	1.29	77	0.1354
3	37	40	288	1.29	77	0.1354
4	33	50	301	1.31	96	0.1083
5	32	60	313	1.36	115	0.1054
6	33	60	313	1.36	115	0.1094
7	35	60	313	1.38	115	0.1253
8	31	70	326	1.40	135	0.0981
9	34	70	326	1.42	135	0.1184
10	30	80	338	1.45	154	0.0930

Table 1 – Results of the optimization procedure in the first design phase.

The second phase of the optimization procedure is performed by assuming the same variables and constraints already employed in the first phase. The results are listed in Table 2.

Finally, the search for the sliders optimal position has been performed alongside the elastomeric elements sizing optimization. The search space area is limited to a single rack size equal to 800 mm × 1000 mm. The minimum number of sliders required for an equilibrium configuration is three. In this study, the 4-slider scheme is also investigated.

Isolator diameter [mm]	Total rubber thickness [mm]	Cost of isolation system [€]	Objective function	Max seismic displacement [mm]	Max acceleration isolated rack [g]
30	80	338	1.45	154	0.0930

Table 2 – Results of the optimization procedure in the second design phase.

Figure 6 shows all feasible positions generated by the differential evolution algorithm during the optimization process in case of 4 sliders (color intensity indicates the age of the sliders' candidate positions during the optimization procedure, which means that lighter dots indicate earlier generations than darker ones). The final results for both the 4-sliders and 3-sliders problems are shown in Figure 7.

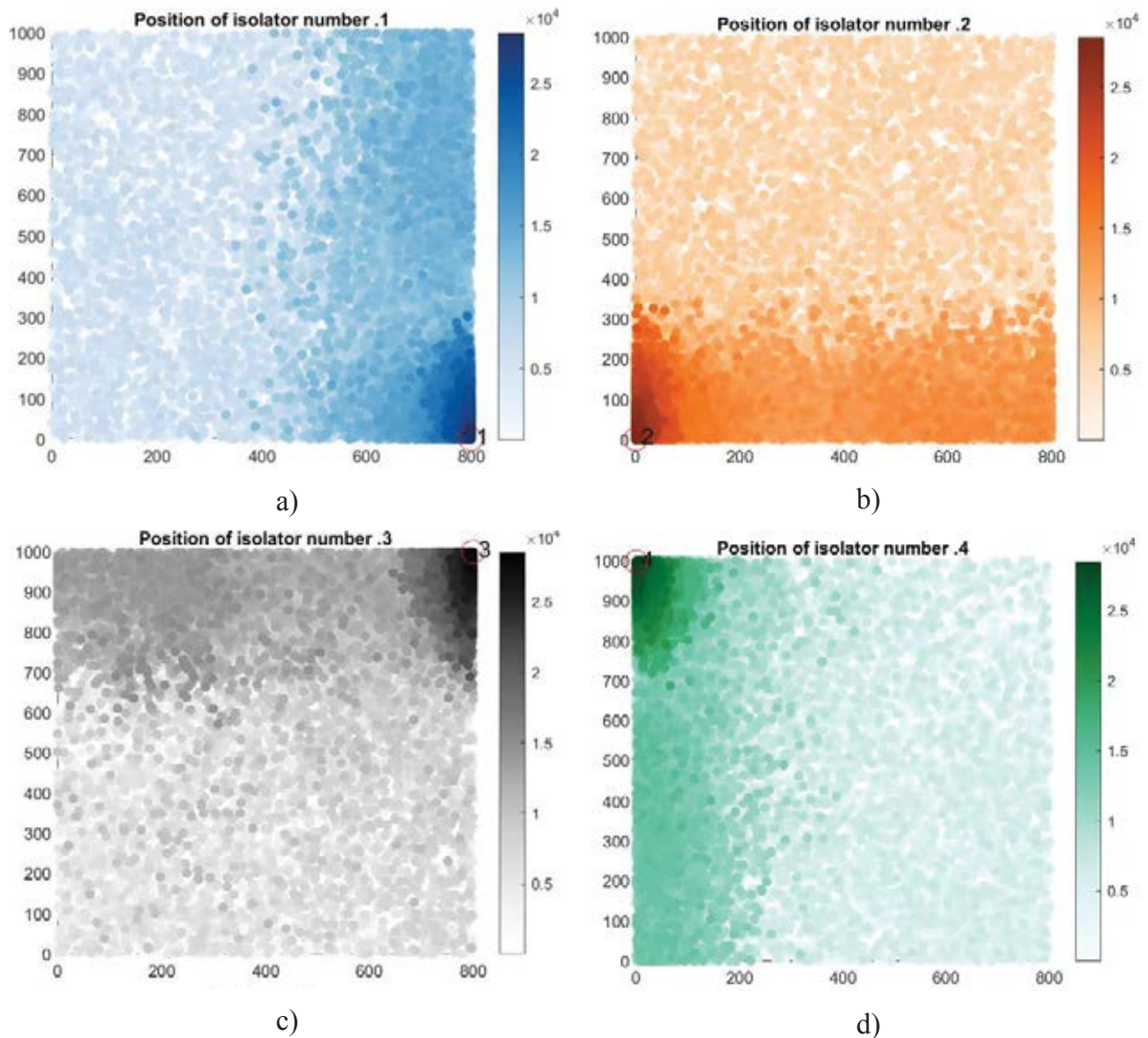


Figure 6 – Position of the sliders during the optimization procedure (the color gradient indicates the position during the evolutionary search): a) position of slider number 1; b) position of slider number 2; c) position of slider number 3; d) position of slider number 4.

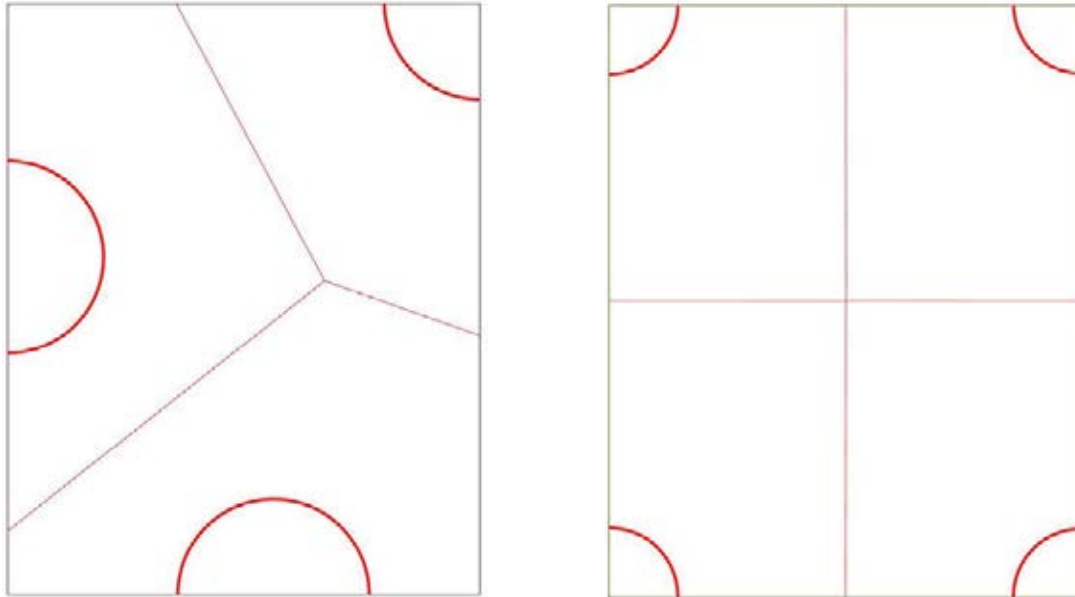


Figure 7 – Optimal positions of the sliders in case of 3 (left) or 4 (right) devices.

7 CONCLUSIONS

This paper has explored the application of the constrained differential evolution algorithm for the optimum and standardized design of a hybrid seismic isolation device for a server rack. The device is designed in compliance with EN 15129 and EN 1337-3. Size of the elastomeric devices and positions of the sliders have been optimized.

The sizing optimization of elastomeric devices allow to draw the following general conclusions:

- the most important seismic demand parameter for the integrity of the elastomeric isolators is the lateral seismic displacement, which increases as the number of floors grows up and ultimately governs the total height of the device;
- the isolator diameter is almost constant for all buildings under consideration and is close to the lower bound of the search space;
- the optimum design of the isolation system performed taking into account all buildings simultaneously leads to the same results carried out considering the tallest building only, which therefore rules the whole design because of the largest value of the seismic demand.

As regards the sliders position, an intuitive layout is obtained for the configuration consisting of 4 devices, whereas the optimal arrangement for 3 devices is less predictable.

The optimization of the isolation system has been here performed through a constrained differential evolution algorithm. This numerical technique was able to reduce the total computational time and to provide a better solution as compared to a parametric analysis-aided approach. Therefore, the constrained differential evolution algorithm proved to be suitable for this optimization problem.

The design procedure herein proposed will be further extended in future works so as to enable the optimization of the other racks configurations typically encountered in data centers.

REFERENCES

- [1] R. Villaverde, Seismic Design of Secondary Structures: State of the Art, J. Struct. Eng.

- 123 (1997) 1011–1019. [https://doi.org/10.1061/\(asce\)0733-9445\(1997\)123:8\(1011\)](https://doi.org/10.1061/(asce)0733-9445(1997)123:8(1011)).
- [2] C. Alhan, H.P. Gavin, Reliability of base isolation for the protection of critical equipment from earthquake hazards, *Eng. Struct.* 27 (2005) 1435–1449. <https://doi.org/10.1016/j.engstruct.2005.04.007>.
- [3] S. Taghavi, E. Miranda, Response Assessment of Nonstructural Building Elements, *Pacific Earthq. Eng. Res.* (2003) 96.
- [4] E. Makwae, An assessment of disaster recovery planning: A strategy for data security, Researchgate. (2018).
- [5] G. Quaranta, W. Lacarbonara, S.F. Masri, A review on computational intelligence for identification of nonlinear dynamical systems, Springer Netherlands, 2020. <https://doi.org/10.1007/s11071-019-05430-7>.
- [6] F.F. Tajirian, SEISMIC VULNERABILITY OF DATA CENTERS, in: 2009: pp. 616–626.
- [7] M.K. Patterson, D.G. Costello, P.F. Grimm, M. Loeffler, Data center TCO ; a comparison of high-density and low-density spaces, *Chart.* (2007) 1–12. <http://www.pentium.ch/technology/eep/datacenter.pdf>.
- [8] W. Lintner, B. Tschudi, O. VanGeet, Best Practices Guide for Energy-Efficient Data Center Design, U.S Dep. Energy. (2011) i–24. <http://www1.eere.energy.gov/femp/pdfs/eedatacenterbestpractices.pdf>.
- [9] H. Geng, Data Center Handbook, 2014. <https://doi.org/10.1002/9781118937563>.
- [10] N. Rasmussen, Guidelines for Specification of Data Center Power Density, APC White Pap. #120. (2005) 1–21.
- [11] THK, Seismic Isolation Module Model TGS, Japan, Japan, n.d.
- [12] THK, Seismic Isolation Table Model TSD, Japan, n.d.
- [13] DIS, Non-Structural Isolation - DIS Catalogue, McCarran, Nevada, n.d. www.dis-inc.com.
- [14] P.S. Harvey, H.P. Gavin, Double rolling isolation systems: A mathematical model and experimental validation, *Int. J. Non. Linear. Mech.* 61 (2014) 80–92. <https://doi.org/10.1016/j.ijnonlinmec.2014.01.011>.
- [15] M. Nacamuli, Seismic protection of data centers using Ball-N-cone base isolation, *Struct. Congr. 2012 - Proc. 2012 Struct. Congr.* (2012) 1373–1384. <https://doi.org/10.1061/9780784412367.123>.
- [16] MAURER, Maurer Vibration Isolation Catalogue, n.d.
- [17] Mu-Solator, Mu-Solator DataCenter - Catalogue, 2019.
- [18] Mu-Solator, Mu-Solator Server Rack - Catalogue, 2019.
- [19] LG Earthquake Defense, Seismic Isolation for Machines - LG Catalogue, n.d.
- [20] LG Earthquake Defense, Seismic Mount for Data Centers, n.d.
- [21] I.-K. Chang, S.-C. Liu, H.C. Shah, Seismic support of electronic and computer equipment on raised floors, *Soil Dyn. Earthq. Eng.* 5 (1986) 159–169. [https://doi.org/10.1016/0267-7261\(86\)90019-9](https://doi.org/10.1016/0267-7261(86)90019-9).

- [22] LG Earthquake Defense, Interstory Isolation For Buildings, n.d.
- [23] A. Filiatrault, P.S. Higgins, A. Wanitkorkul, J.A. Courtwright, R. Michael, Experimental seismic response of base isolated pallet-type steel storage racks, *Earthq. Spectra*. 24 (2008) 617–639. <https://doi.org/10.1193/1.2942375>.
- [24] F. 461, FEMA 461 / June 2007, (2007).
- [25] S. Committee of the IEEE Power Engineering Society, IEEE Std 693TM-2005 (Revision of IEEE Std 693-1997) IEEE Recommended Practice for Seismic Design of Substations, 2006.
- [26] JIS C6011-2-2011 JIS C6010, (n.d.).
- [27] N. Equipment, P. Grounding, ATT-TP-76200, 14 (2016) 1–73.
- [28] D. Version, N.O.T.F.O.R. Resale, ANSI/BICSI 002-2014 - Data Center Design and Implementation Best Practices, (2014).
- [29] Telcordia Technologies Generic Requirements, NEBS TM Requirements: Physical ProtectTelcordia Technologies Generic Requirements GR-63-CORE Issue 4, 2012. <http://telecom-info.telcordia.com>. (accessed April 21, 2020).
- [30] C. DiMinico, Telecommunications Infrastructure Standard for Data Centers, *MC Commun.* (2010) 36.
- [31] E. Miranda, G. Mosqueda, R. Retamales, G. Pekcan, Performance of nonstructural components during the 27 February 2010 Chile earthquake, *Earthq. Spectra*. 28 (2012) 453–471. <https://doi.org/10.1193/1.4000032>.
- [32] CEN, EN 15129:2018 - Anti-seismic devices, (2018).
- [33] CEN, EN 1337-3 - Structural bearings - Part 3: Elastomeric bearings, (2005).
- [34] P.M. Calvi, Relative displacement floor spectra for seismic design of non structural elements, *J. Earthq. Eng.* 18 (2014) 1037–1059. <https://doi.org/10.1080/13632469.2014.923795>.
- [35] Ministero delle Infrastrutture e dei Trasporti, Aggiornamento delle “Norme tecniche per le costruzioni” (in Italian), (2018) 1–198.
- [36] A. Scodreggio, G. Quaranta, G.C. Marano, G. Monti, R.B. Fleischman, Optimization of force-limiting seismic devices connecting structural subsystems, *Comput. Struct.* 162 (2016) 16–27. <https://doi.org/10.1016/j.compstruc.2015.09.008>.
- [37] G. Quaranta, A. Fiore, G.C. Marano, Optimum design of prestressed concrete beams using constrained differential evolution algorithm, *Struct. Multidiscip. Optim.* 49 (2014) 441–453. <https://doi.org/10.1007/s00158-013-0979-5>.
- [38] S. Canfield, Seismic Evaluation of Large Server Computer Structure, (2016) 1–6.